

Thermal Willis Coupling in Spatiotemporal Diffusive Metamaterials

Liujun Xu,^{1,2} Guoqiang Xu,¹ Jiaxin Li,¹ Ying Li,^{3,4} Jiping Huang^{1b,2,*} and Cheng-Wei Qiu^{1b,†}

¹*Department of Electrical and Computer Engineering, National University of Singapore, Singapore 117583, Singapore*

²*Department of Physics, State Key Laboratory of Surface Physics, and Key Laboratory of Micro and Nano Photonic Structures (MOE), Fudan University, Shanghai 200438, China*

³*Interdisciplinary Center for Quantum Information, State Key Laboratory of Modern Optical Instrumentation, ZJU-Hangzhou Global Scientific and Technological Innovation Center, Zhejiang University, Hangzhou 310027, China*

⁴*International Joint Innovation Center, Key Laboratory of Advanced Micro/Nano Electronic Devices & Smart Systems of Zhejiang, The Electromagnetics Academy of Zhejiang University, Zhejiang University, Haining 314400, China*

 (Received 14 February 2022; accepted 19 September 2022; published 7 October 2022)

Willis coupling generically stems from bianisotropy or chirality in wave systems. Nevertheless, those schemes are naturally unavailable in diffusion systems described by a single constitutive relation governed by the Fourier law. Here, we report spatiotemporal diffusive metamaterials by modulating thermal conductivity and mass density in heat transfer. The Fourier law should be modified after homogenizing spatiotemporal parameters, featuring thermal Willis coupling between heat flux and temperature change rate. Thermal Willis coupling drives asymmetric heat diffusion, and the diffusion direction is reversible at a critical point determined by the degree of spatiotemporal modulation. Moreover, thermal Willis coupling stands robustly even when only thermal conductivity is modulated. These results may have potential applications for directional diffusion and offer insights into asymmetric manipulation of nonequilibrium mass and energy transfer.

DOI: [10.1103/PhysRevLett.129.155901](https://doi.org/10.1103/PhysRevLett.129.155901)

Since the theory of transformation thermotics [1,2] was proposed, various thermal metamaterials [3–5] have been designed to realize cloaking and camouflaging functions [6–8] based on artificial structures with spatially distributed parameters. However, those schemes are insufficient to break the inherent space-inversion symmetry of thermal conduction. Asymmetric diffusion is crucial for heat collection and storage. For example, the ambient temperature during the day is relatively high, and the device allows heat to diffuse inward. In contrast, the device hinders heat from diffusing outward at night with relatively low ambient temperature. With temporal modulation developing in electromagnetic [9–12] and acoustic [13,14] systems, it has also been introduced to diffusion systems [15–18], providing an insightful paradigm to achieve asymmetric diffusion by spatiotemporal modulation. Nevertheless, unlike the electric counterpart [18], the spatiotemporal modulation of mass density generates local advection heat flux because mass conservation should be carefully considered. Consequently, heat transfer becomes symmetric again with the requirement of mass conservation [19], making it elusive to uncover asymmetric heat transfer in spatiotemporal diffusion systems.

On the other hand, Willis coupling in acoustic and elastic systems features two nonzero off-diagonal components in the two-dimensional matrix [20–25], also corresponding to magnetoelectric coupling in electromagnetic systems [26,27]. Since Willis coupling results from high-order

perturbations that are insufficient for apparent phenomena, many efforts have been made to maximize Willis coupling [28–30] and reveal nonreciprocal properties [31–34]. However, those schemes for Willis coupling [20–34] are naturally unavailable in diffusion systems, making it extremely difficult to achieve asymmetric heat diffusion by the modified Fourier law.

Here, we propose the concept of Willis thermal metamaterials by spatiotemporal modulation, featuring thermal Willis coupling between heat flux and temperature change rate. Restricted by the intrinsic space-inversion symmetry of thermal conduction, the temperature field velocity of v is zero in conventional thermal materials [Fig. 1(a)]. Temperature field propagation means the movement of a wavelike temperature profile [35–39]. In contrast, Willis thermal metamaterials drive directional temperature field propagation [Fig. 1(a)], exhibiting asymmetric diffusion feature [40–44]. Intriguingly, the propagating direction is reversible at a critical point of the modulation velocity of u , and $v > 0$, $v = 0$, and $v < 0$ are realized at will [Figs. 1(a) and 1(b)]. The direction reversal implies that the present asymmetry results from high-order perturbations, in contrast to the reported asymmetry induced by the first-order advectionlike effect, whose direction is generally the same as the modulation direction [15]. We first discuss a generalized model with spatiotemporal modulation of mass density and thermal conductivity [Fig. 1(c)]. The model is further simplified by modulating only thermal conductivity

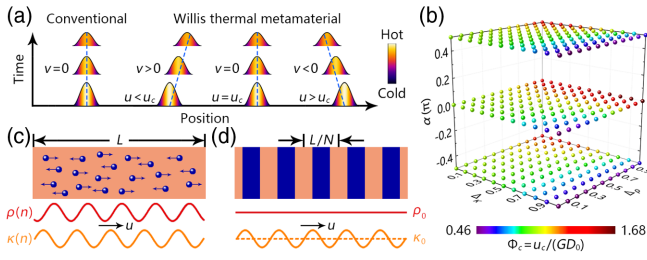


FIG. 1. Schematic of asymmetric heat diffusion. (a) In contrast to the conventional case with a zero velocity of temperature field propagation, i.e., $v = 0$, Willis thermal metamaterials drive directional temperature field propagation. The propagating direction is determined by a critical point of the modulation velocity of u , i.e., u_c . (b) For generality, we make u_c dimensionless by defining the dimensionless parameter of $\Phi_c = u_c / (GD_0)$. The critical point of Φ_c only depends on the modulation amplitudes of Δ_ρ and Δ_κ and the modulation phase difference of α . (c) Generalized model by modulating mass density of $\rho(n)$ and thermal conductivity of $\kappa(n)$ with $n = x - ut$. The modulation of mass density produces local advection heat flux. (d) Simplified model by modulating only thermal conductivity.

[Fig. 1(d)], again distinguishing our work from the existing research where a two-parameter modulation is mandatory [15–18].

One-dimensional thermal conduction in a homogeneous medium is governed by $\rho_0 C_0 \partial_t T + \partial_x (-\kappa_0 \partial_x T) = 0$, where ρ_0 , C_0 , and κ_0 are the mass density, heat capacity, and thermal conductivity of the homogeneous medium. We consider spatiotemporal modulation of mass density and thermal conductivity,

$$\rho(n) = \rho_0 [1 + \Delta_\rho \cos(Gn + \alpha)], \quad (1a)$$

$$\kappa(n) = \kappa_0 [1 + \Delta_\kappa \cos(Gn)], \quad (1b)$$

where Δ_ρ and Δ_κ denote the modulation amplitudes, α is the modulation phase difference, $G = 2\pi N/L$ represents the modulation wave number, L is the length, N is the period number, and $n = x - ut$ is the generalized coordinate. The diffusion equation describes classical and macroscopic heat transfer. Hence, for the validity of the diffusion equation, the spatial modulation scale should be much larger than the mean free path of heat carriers, and the temporal modulation scale should also be much longer than the relaxation time of colliding events. Then, one-dimensional heat transfer with spatiotemporal modulation is governed by

$$\rho(n) C_0 \frac{\partial T}{\partial t} + u [\rho(n) - \rho_0] C_0 \frac{\partial T}{\partial x} + \frac{\partial}{\partial x} \left(-\kappa(n) \frac{\partial T}{\partial x} \right) = 0. \quad (2)$$

A local advection term of $u [\rho(n) - \rho_0] C_0 \partial_x T$ appears due to mass conservation [19]. Nevertheless, its integration over one period is still zero, and thus there is no macroscopically

directional advection in the system (see Part I of Supplemental Material [45]).

We then homogenize Eq. (2) by considering a wavelike temperature solution with the Floquet-Bloch theorem,

$$T = \epsilon(n) e^{i(\beta x - \omega t)} + T_0 = \left(\sum_s \epsilon_s e^{isGn} \right) e^{i(\beta x - \omega t)} + T_0, \quad (3)$$

where β and ω are the wave number and frequency of the wavelike temperature field. ω is a complex number whose imaginary part indicates the temporal decay of the variation amplitude of the wavelike temperature field. Hence, the system finally goes to a constant temperature, i.e., $T = T_0$. Without loss of generality, the balanced temperature of T_0 is set at zero degrees kelvin, and the real part of Eq. (3) makes sense. $\epsilon(n)$ is the Floquet-Bloch modulation function with $s = 0, \pm 1, \pm 2, \dots, \pm \infty$ and $\epsilon_0 = 1$. We ensure the accuracy of numerical results by considering the order of s as high as possible. Nevertheless, it is not intuitive to uncover the physical mechanism, and thus we only take $s = 0, \pm 1$ for analytical discussion. We also assume $\beta \ll G$ to ensure a subwavelength structure, i.e., the structural unit size is far smaller than the temperature field wavelength. Hence, our structure belongs to metamaterials, and homogenization makes sense. The homogenized heat transfer equation is

$$\rho_0 C_0 \frac{\partial T_0}{\partial t} - K \frac{\partial^2 T_0}{\partial x^2} - R \frac{\partial^2 T_0}{\partial t^2} - W \frac{\partial^2 T_0}{\partial t \partial x} = 0, \quad (4)$$

where $T_0 = e^{i(\beta x - \omega t)}$ is the homogenized temperature (see Part II of Supplemental Material [45]). The homogenized parameters are

$$K = \kappa_0 \left(1 + \frac{-\Delta_\kappa^2 + \Delta_\rho^2 \Phi^2 + 2\Delta_\kappa \Delta_\rho \Phi^2 \cos \alpha}{2(1 + \Phi^2)} \right), \quad (5a)$$

$$R = \frac{\kappa_0}{u^2} \frac{\Delta_\rho^2 \Phi^2}{2(1 + \Phi^2)}, \quad (5b)$$

$$W = \frac{\kappa_0}{u} \frac{\Delta_\rho^2 \Phi^2 + \Delta_\kappa \Delta_\rho \Phi^2 \cos \alpha}{1 + \Phi^2}, \quad (5c)$$

with definitions of the dimensionless parameter of $\Phi = u / (GD_0) = uL / (2\pi ND_0)$ and thermal diffusivity of $D_0 = \kappa_0 / (\rho_0 C_0)$. The status of Δ_ρ and Δ_κ is, to some extent, different in Eq. (5c) because mass conservation should be seriously considered. Heat transfer in spatiotemporal diffusive metamaterials can no longer be homogenized within the framework of thermal conduction due to the two unexpected terms of ∂_t^2 and $\partial_t \partial_x$ in Eq. (4). As energy conservation indicates, the universal heat conduction equation in one dimension is $\rho_0 C_0 \partial_t T_0 + \partial_x J = 0$, where J is the heat flux. Comparing the energy conservation equation and Eq. (4), we should modify the Fourier law as

$$-\frac{R}{\rho_0 C_0} \frac{\partial J}{\partial t} + J = -K \frac{\partial T_0}{\partial x} - W \frac{\partial T_0}{\partial t}. \quad (6)$$

The term of $\partial_t J$ is mathematically related to thermal relaxation [37], the term of $\partial_x T_0$ reflects the conventional contribution of thermal conduction, and the term of $\partial_t T_0$ is referred to as the thermal Willis term (see Part III of Supplemental Material [45]). Therefore, thermal Willis coupling originates from the coupling between heat flux and temperature change rate. This effect is similar to acoustic Willis coupling, i.e., acoustic propagation in inhomogeneous media cannot be described by the classical elastic wave equation [20]. Although Eq. (6) directly indicates thermal Willis coupling, it is obtained from two approximations of $s = 0, \pm 1$ and $\beta \ll G$. Therefore, Eq. (6) is not strictly accurate, but this problem is solved by exploring numerical results.

A remarkable feature that distinguishes Willis thermal metamaterials from conventional thermal materials is the ability to drive asymmetric heat diffusion [Fig. 1(a)]. The frequency of ω is purely imaginary in homogeneous media, making the propagation velocity of $v = \text{Re}[\omega]/\beta$ zero (see Part IV of Supplemental Material [45]). In contrast, Willis thermal metamaterials realize directional temperature field propagation because the real part of ω appears. To avoid the probable inaccuracy of Eq. (4), we study numerical results by considering $s = 0, \pm 1, \pm 2, \dots, \pm 8$ (see Part IV of Supplemental Material [45]). We further explore the six crucial parameters of $u, D_0, N, \Delta_\rho, \Delta_\kappa$, and α in Eq. (1) that affect the velocity of $v = \text{Re}[\omega]/\beta$ and temporal decay rate of $\mu = -\text{Im}[\omega]$. These six parameters are divided into two groups. One group contains u, D_0 , and N , linked by the dimensionless parameter of $\Phi = u/(GD_0)$ or $2\pi\Phi = uL/(ND_0)$. Specifically, Φ has a critical point of Φ_c , crossing which the temperature field direction is reversed. The other group includes $\Delta_\rho, \Delta_\kappa$, and α , determining the value of Φ_c [Fig. 1(b)].

We first discuss the former group related to $2\pi\Phi = uL/(ND_0)$. When we set $2\pi\Phi$ as the abscissa, the actual variable is u which is flexibly controllable [Figs. 2(a) and 2(b)]. All $v - 2\pi\Phi$ curves experience a process to be first positive and then negative, but the modulation velocity of u is always positive, exhibiting unexpected direction-reversible heat diffusion. These $v - 2\pi\Phi$ curves also share the same critical point of $2\pi\Phi_c = 6.4$ [stars in Figs. 2(a) and 2(b)]. Accordingly, the maximum (or minimum) values appear at the same value of $2\pi\Phi$ [vertical dashed lines in Figs. 2(a) and 2(b)]. The amplitude of a $v - 2\pi\Phi$ curve is determined by the thermal diffusivity of D_0 and period number of N . Specifically, a larger D_0 (reflected in the dimensionless thermal diffusivity of $M = D_0/D_r$ where D_r is the reference thermal diffusivity) or a smaller N contributes to a larger amplitude. Since the temporal decay rate of μ mainly depends on the effective thermal diffusivity, the $\mu - 2\pi\Phi$

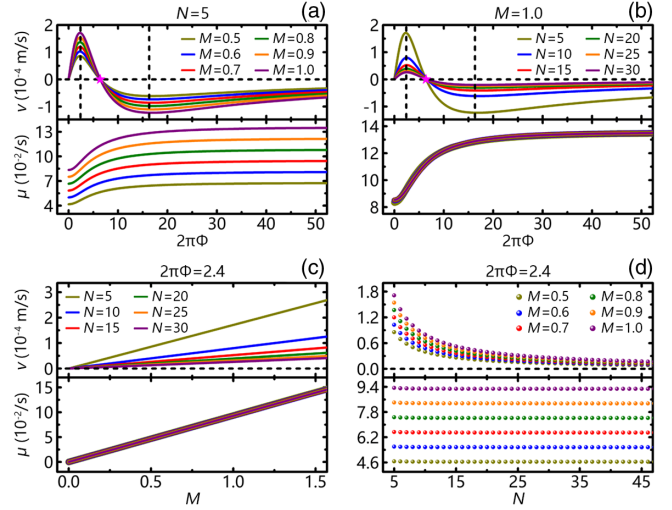


FIG. 2. Numerical results of asymmetric heat diffusion. Velocity of $v = \text{Re}[\omega]/\beta$ and temporal decay rate of $\mu = -\text{Im}[\omega]$ as a function of (a) and (b) dimensionless parameter of $2\pi\Phi = uL/(NMD_r)$, (c) dimensionless thermal diffusivity of $M = D_0/D_r$, and (d) period number of N , where D_r is the reference thermal diffusivity. Except for the parameters shown in each inset, the others are $\Delta_\rho = 0.5$, $\Delta_\kappa = 0.5$, $\alpha = 0$, $D_r = 10^{-4} \text{ m}^2/\text{s}$, and $L = 0.2 \text{ m}$.

curves in Fig. 2(a) have different amplitudes because of the different thermal diffusivity of D_0 . However, the $\mu - 2\pi\Phi$ curves in Fig. 2(b) are almost overlapped because the period number of N essentially does not affect the effective thermal diffusivity. Then we focus on the properties when $2\pi\Phi = 2.4$, corresponding to the maximum values of the $v - 2\pi\Phi$ curves in Figs. 2(a) and 2(b). v and μ demonstrate linear responses to the thermal diffusivity of D_0 [Fig. 2(c)]. Therefore, the temperature field propagation is faster with the larger thermal diffusivity, but the temporal decay rate also becomes larger. The $v - N$ curves decrease in Fig. 2(d), indicating that thermal Willis coupling is weakened with the decrement of inhomogeneity (i.e., the increment of N). The $\mu - N$ curves have almost no variation because the period number of N does not affect the effective thermal diffusivity. In terms of the importance of inhomogeneity, the larger the modulation wavelength (i.e., the smaller N), the more obvious thermal Willis coupling in principle. But we should also ensure that the modulation wavelength is much smaller than the temperature field wavelength so that homogenization makes sense. Therefore, on the premise of guaranteeing good homogenization, the larger the modulation wavelength, the better. More details are provided in Part V of Supplemental Material [45].

We further discuss the latter group related to $\Delta_\rho, \Delta_\kappa$, and α , determining the critical point of $2\pi\Phi_c$. As shown in Figs. 2(a) and 2(b), the critical point for $v = 0$ is fixed at $2\pi\Phi_c = 6.4$, which is irrelevant to thermal diffusivity and period number. Then we discuss the critical point when

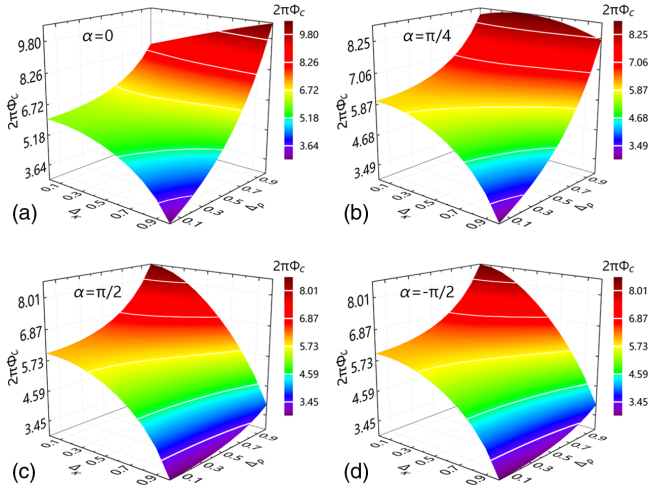


FIG. 3. Critical point of $2\pi\Phi_c = u_c L / (ND_0)$ as a function of the modulation amplitudes of Δ_ρ and Δ_κ . (a)–(d) The modulation phase difference of α takes 0, $\pi/4$, $\pi/2$, and $-\pi/2$. The critical point of $2\pi\Phi_c$ is irrelevant to specific L , N , and D_0 .

$\alpha = 0, \pi/4, \pi/2$, and $-\pi/2$ in Fig. 3. When $\Delta_\rho = 0$ or $\Delta_\kappa = 0$, α does not matter, and hence the $2\pi\Phi_c - \Delta_\rho$ curves with $\Delta_\kappa = 0$ (or the $2\pi\Phi_c - \Delta_\kappa$ curves with $\Delta_\rho = 0$) are identical in Fig. 3. Moreover, $\alpha = \pm\pi/2$ leads to the same patterns of $2\pi\Phi_c$, and hence thermal Willis coupling is an even function of α . The results in Fig. 3 provide direct guidance for designing direction-reversible heat diffusion (see Part V of Supplemental Material [45]).

Another feature of thermal Willis coupling is the freedom from modulating mass density and thermal conductivity simultaneously. It is mandatory to modulate two parameters simultaneously for the reported diffusive asymmetry induced by the advectionlike effect [15–18]. However, the homogenized case described by Eq. (4) does

not contain any advectionlike term. Thermal Willis coupling between heat flux and temperature change rate realizes asymmetry, which works in transient heat transfer rather than quasisteady heat transfer (see Part VI of Supplemental Material [45]). Transient (or quasisteady) heat transfer means that the temperature field envelope is dependent on (or independent of) time. Because of the essential difference, a single-parameter modulation is enough to realize asymmetric diffusion. Since the thermal conductivity of many practical materials is sensitive to external fields [46–48], we may design a moving periodic external field to achieve the spatiotemporal modulation of thermal conductivity [Fig. 1(d)]. Nevertheless, the inaccuracy of Eq. (4) also appears when $\Delta_\rho = 0$. The R in Eq. (5b) and W in Eq. (5c) become zero, yielding $v = 0$. However, the numerical results and following simulations indicate $v \neq 0$. This deviation is understandable because Eq. (4) is obtained using the first-order approximation, i.e., $s = 0, \pm 1$. Therefore, Eq. (4) can prove the absence of the advectionlike term (the first-order effect) but cannot accurately calculate the high-order effects.

Then we discuss the single-parameter modulation of thermal conductivity. We plot the $v - 2\pi\Phi$ curves in Fig. 4(a). As $2\pi\Phi$ (i.e., u) increases, v first increases from zero, decreases to negative values, and finally tends to zero. A larger Δ_κ leads to the larger amplitude of a $v - 2\pi\Phi$ curve. Moreover, μ monotonically increases and finally goes to a constant value [Fig. 4(b)]. The upper limit is $D_0\beta^2$, i.e., the temporal decay rate in a homogeneous medium (see Part V of Supplemental Material [45]). In other words, when $2\pi\Phi \rightarrow \infty$, spatiotemporal modulation does not contribute to any inhomogeneity, indicating no thermal Willis coupling and $v = 0$.

We further perform finite-element simulations with COMSOL Multiphysics and discuss the parameters marked

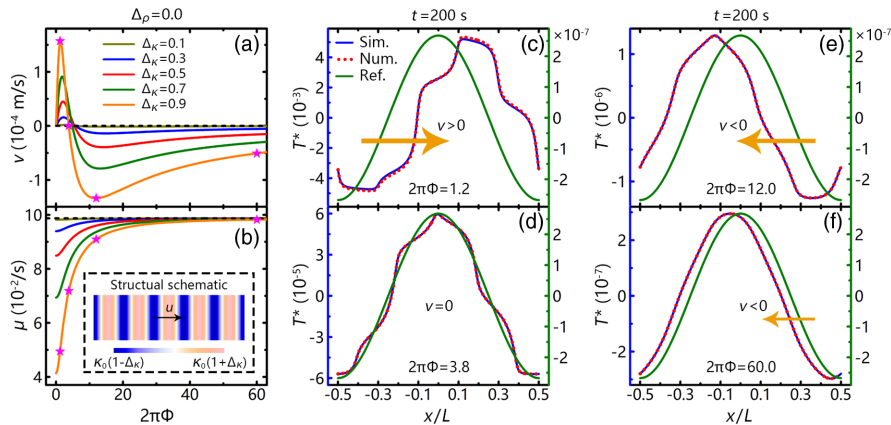


FIG. 4. Simulations of asymmetric heat diffusion by modulating only thermal conductivity. (a) Velocity of $v = \text{Re}[\omega]/\beta$ and (b) temporal decay rate of $\mu = -\text{Im}[\omega]$ as a function of the dimensionless parameter of $2\pi\Phi = uL/(ND_0)$. Dimensionless temperature distributions of T^* at 200 s with (c) $2\pi\Phi = 1.2$, (d) $2\pi\Phi = 3.8$, (e) $2\pi\Phi = 12.0$, and (f) $2\pi\Phi = 60.0$. The initial dimensionless temperature is $T^* = 100 \cos(2\pi x/L)$. The left and right boundaries are set with periodic conditions, i.e., continuous temperatures. Parameters: $D_0 = 10^{-4} \text{ m}^2/\text{s}$, $L = 0.2 \text{ m}$, and $N = 5$. Sim.: Simulation; Num.: Numerical; and Ref.: Reference.

by stars in Figs. 4(a) and 4(b). The thermal conductivity is set according to Eq. (2b) for quantitative comparison with the theory and numerical results. For brevity, we define a dimensionless temperature as $T^* = (T - T_0)/(1 \text{ K})$. The wavelike temperature profile for reference is stationary and only decays. In contrast, the spatiotemporal modulation of thermal conductivity drives forward temperature field propagation [Fig. 4(c)]. At the critical point of $2\pi\Phi = 3.8$, despite a nonzero modulation velocity of u , the temperature field velocity is still zero [Fig. 4(d)]. The further increment of $2\pi\Phi$ leads to backward temperature field propagation [Figs. 4(e) and 4(f)]. Moreover, the numerical results also agree well with the simulations, convincing the results in Figs. 2 and 3.

For experimental demonstration, we suggest a practical model with square-wave modulation (see Part VII of Supplemental Material [45]). Meanwhile, we discuss the modulation efficiency by defining $\eta = v/u$ to reflect the strength of temperature field response to spatiotemporal modulation, guiding the parameter design in experiments (see Part VII of Supplemental Material [45]).

In summary, the constitutive relation determined by the Fourier law should be modified after homogenizing spatiotemporal inhomogeneity, manifesting as thermal Willis coupling between heat flux and temperature change rate. Then we design Willis thermal metamaterials to uncover asymmetric heat diffusion, with a critical point determining the diffusion direction reversal. Thermal Willis coupling is particularly robust even with the single-parameter modulation of thermal conductivity. The relaxed requirement makes it possible to extend our mechanism for heat diffusion to other energy and mass diffusion systems, such as particle diffusion [49,50] and light diffusion [51,52], where only diffusivity is controllable. Since Willis thermal metamaterials are almost irrelevant to specific scales and temperatures, they could be widely applied for realizing asymmetric diffusion of energy and mass.

C.-W. Q. acknowledges the support from the Singapore Ministry of Education (Grant No. A-8000107-01-00). J. H. acknowledges the support from the National Natural Science Foundation of China (Grants No. 11725521 and No. 12035004) and the Science and Technology Commission of Shanghai Municipality (Grant No. 20JC1414700). Y. L. acknowledges the support from the National Natural Science Foundation of China (Grant No. 92163123).

*jphuang@fudan.edu.cn

†chengwei.qiu@nus.edu.sg

- [1] C. Z. Fan, Y. Gao, and J. P. Huang, *Appl. Phys. Lett.* **92**, 251907 (2008).
 [2] T. Y. Chen, C.-N. Weng, and J.-S. Chen, *Appl. Phys. Lett.* **93**, 114103 (2008).

- [3] J. P. Huang, *Theoretical Thermotics: Transformation Thermotics and Extended Theories for Thermal Metamaterials* (Springer, Singapore, 2020).
 [4] S. Yang, J. Wang, G. L. Dai, F. B. Yang, and J. P. Huang, *Phys. Rep.* **908**, 1 (2021).
 [5] Y. Li, W. Li, T. C. Han, X. Zheng, J. X. Li, B. W. Li, S. H. Fan, and C.-W. Qiu, *Nat. Rev. Mater.* **6**, 488 (2021).
 [6] Y. Li, K.-J. Zhu, Y.-G. Peng, W. Li, T. Z. Yang, H. X. Xu, H. Chen, X.-F. Zhu, S. H. Fan, and C.-W. Qiu, *Nat. Mater.* **18**, 48 (2019).
 [7] G. Q. Xu, K. C. Dong, Y. Li, H. G. Li, K. P. Liu, L. Q. Li, J. Q. Wu, and C.-W. Qiu, *Nat. Commun.* **11**, 6028 (2020).
 [8] R. Hu, W. Xi, Y. D. Liu, K. C. Tang, J. L. Song, X. B. Luo, J. Q. Wu, and C.-W. Qiu, *Mater. Today* **45**, 120 (2021).
 [9] N. Engheta, *Nanophotonics* **10**, 639 (2021).
 [10] D. Torrent, *Phys. Rev. B* **102**, 214202 (2020).
 [11] V. Pacheco-Peña and N. Engheta, *New J. Phys.* **23**, 095006 (2021).
 [12] D. M. Solís and N. Engheta, *Phys. Rev. B* **103**, 144303 (2021).
 [13] D. Torrent, W. J. Parnell, and A. N. Norris, *Phys. Rev. B* **97**, 014105 (2018).
 [14] X. H. Wen, X. H. Zhu, H. W. Wu, and J. Li, *Phys. Rev. B* **104**, L060304 (2021).
 [15] D. Torrent, O. Poncelet, and J.-C. Batsale, *Phys. Rev. Lett.* **120**, 125501 (2018).
 [16] L. J. Xu, J. P. Huang, and X. P. Ouyang, *Phys. Rev. E* **103**, 032128 (2021).
 [17] J. Ordóñez-Miranda, Y. Y. Guo, J. J. Alvarado-Gil, S. Volz, and M. Nomura, *Phys. Rev. Appl.* **16**, L041002 (2021).
 [18] M. Camacho, B. Edwards, and N. Engheta, *Nat. Commun.* **11**, 3733 (2020).
 [19] J. X. Li, Y. Li, P.-C. Cao, M. H. Qi, X. Zheng, Y.-G. Peng, B. W. Li, X.-F. Zhu, A. Alù, and C.-W. Qiu, *Nat. Commun.* **13**, 167 (2022).
 [20] J. R. Willis, *Wave Motion* **3**, 1 (1981).
 [21] G. W. Milton and J. R. Willis, *Proc. R. Soc. A* **463**, 855 (2007).
 [22] M. B. Muhlestein, C. F. Sieck, A. Alù, and M. R. Haberman, *Proc. R. Soc. A* **472**, 20160604 (2016).
 [23] C. F. Sieck, A. Alù, and M. R. Haberman, *Phys. Rev. B* **96**, 104303 (2017).
 [24] J.-P. Groby, M. Malléjac, A. Merkel, V. Romero-García, V. Tournat, D. Torrent, and J. Li, *New J. Phys.* **23**, 053020 (2021).
 [25] Y. Meng, Y. R. Hao, S. Guenneau, S. B. Wang, and J. Li, *New J. Phys.* **23**, 073004 (2021).
 [26] R. Marqués, F. Medina, and R. Rafii-El-Idrissi, *Phys. Rev. B* **65**, 144440 (2002).
 [27] S. Zhang, Y. S. Park, J. Li, X. Lu, W. Zhang, and X. Zhang, *Phys. Rev. Lett.* **102**, 023901 (2009).
 [28] L. Quan, Y. Ra'di, D. L. Sounas, and A. Alù, *Phys. Rev. Lett.* **120**, 254301 (2018).
 [29] A. Melnikov, Y. K. Chiang, L. Quan, S. Oberst, A. Alù, S. Marburg, and D. Powell, *Nat. Commun.* **10**, 3148 (2019).
 [30] Y. Q. Liu, Z. X. Liang, J. Zhu, L. B. Xia, O. Mondain-Monval, T. Brunet, A. Alù, and J. Li, *Phys. Rev. X* **9**, 011040 (2019).

- [31] L. Quan, D. L. Sounas, and A. Alù, *Phys. Rev. Lett.* **123**, 064301 (2019).
- [32] L. Quan, S. Yves, Y. G. Peng, H. Esfahlani, and A. Alù, *Nat. Commun.* **12**, 2615 (2021).
- [33] C. Cho, X. H. Wen, N. Park, and J. Li, *Communications in Physics* **4**, 82 (2021).
- [34] C. Olivier, G. Poignand, M. Malléjac, V. Romero-García, G. Penelet, A. Merkel, D. Torrent, J. Li, J. Christensen, and J.-P. Groby, *Phys. Rev. B* **104**, 184109 (2021).
- [35] M. Maldovan, *Phys. Rev. Lett.* **110**, 025902 (2013).
- [36] Y. Li, Y.-G. Peng, L. Han, M.-A. Miri, W. Li, M. Xiao, X.-F. Zhu, J. L. Zhao, A. Alù, S. H. Fan, and C.-W. Qiu, *Science* **364**, 170 (2019).
- [37] M. Gandolfi, C. Giannetti, and F. Banfi, *Phys. Rev. Lett.* **125**, 265901 (2020).
- [38] G. Mazza, M. Gandolfi, M. Capone, F. Banfi, and C. Giannetti, *Nat. Commun.* **12**, 6904 (2021).
- [39] G. Q. Xu, Y. Li, W. Li, S. H. Fan, and C.-W. Qiu, *Phys. Rev. Lett.* **127**, 105901 (2021).
- [40] Y. Li, X. Y. Shen, Z. H. Wu, J. Y. Huang, Y. X. Chen, Y. S. Ni, and J. P. Huang, *Phys. Rev. Lett.* **115**, 195503 (2015).
- [41] Y. Li, J. X. Li, M. H. Qi, C.-W. Qiu, and H. S. Chen, *Phys. Rev. B* **103**, 014307 (2021).
- [42] L. J. Xu, J. P. Huang, and X. P. Ouyang, *Appl. Phys. Lett.* **118**, 221902 (2021).
- [43] T. J. Shimokusu, Q. Zhu, N. Rivera, and G. Wehmeyer, *Int. J. Heat Mass Transfer* **182**, 122035 (2022).
- [44] L. J. Xu, G. Q. Xu, J. P. Huang, and C.-W. Qiu, *Phys. Rev. Lett.* **128**, 145901 (2022).
- [45] See Supplemental Material at <http://link.aps.org/supplemental/10.1103/PhysRevLett.129.155901> for detailed discussions.
- [46] X. Y. Shen, Y. Li, C. R. Jiang, and J. P. Huang, *Phys. Rev. Lett.* **117**, 055501 (2016).
- [47] J. Shin, J. Sung, M. Kang, X. Xie, B. Lee, K. M. Lee, T. J. White, C. Leal, N. R. Sottos, P. V. Braun, and D. G. Cahill, *Proc. Natl. Acad. Sci. U.S.A.* **116**, 5973 (2019).
- [48] S. C. Deng, J. L. Yuan, Y. L. Lin, X. X. Yu, D. K. Ma, Y. W. Huang, R. C. Ji, G. Z. Zhang, and N. Yang, *Nano Energy* **82**, 105749 (2021).
- [49] J. M. Restrepo-Flórez and M. Maldovan, *Appl. Phys. Lett.* **111**, 071903 (2017).
- [50] J. M. Restrepo-Flórez and M. Maldovan, *J. Membr. Sci.* **566**, 301 (2018).
- [51] B. Orazbayev, M. Beruete, A. Martínez, and C. García-Meca, *Phys. Rev. A* **94**, 063850 (2016).
- [52] Z. G. Chen and M. Segev, *eLight* **1**, 2 (2021).